

PHYSICAL REVIEW C

NUCLEAR PHYSICS

THIRD SERIES, VOLUME 39, NUMBER 5

MAY 1989

${}^2\text{H}(\vec{d}, \gamma){}^4\text{He}$ reaction at $E_d = 95$ MeV

W. K. Pitts,* H. O. Meyer, L. C. Bland, J. D. Brown,[†] R. C. Byrd,[‡] M. Hugi,[§]
H. J. Karwowski,** P. Schwandt, A. Sinha,^{††} J. Sowinski, and I. J. van Heerden^{‡‡}

Indiana University Cyclotron Facility, Bloomington, Indiana 47405

(Received 6 September 1988)

The tensor analyzing power $A_{yy}(\theta)$, vector analyzing power $A_y(\theta)$, and cross section $\sigma(\theta)$ of the ${}^2\text{H}(\vec{d}, \gamma){}^4\text{He}$ reaction have been measured for the angular range of 55° – 149° in the center of mass system at an incident deuteron energy of 95 MeV. The reaction is dominated by the $\langle {}^1D_2 | E2 | {}^1S_0 \rangle$ transition involving the S -state component of ${}^4\text{He}$, as indicated by the approximately $\sin^2\theta$ angular distribution of the cross section. The observed deviation of $\sigma(\theta)$ from this shape is due to either $M2$ strength, tensor force effects, or both. The tensor analyzing power $A_{yy}(\theta)$ is nearly isotropic, with a typical value of approximately 0.3 ± 0.1 . The vector analyzing power A_y is zero within the statistical precision (typically ± 0.2) of this data set, indicating a reduced contribution from $E1$ and $M2$ transitions compared to lower energies. Direct capture calculations in the plane-wave Born approximation do not reproduce even the sign of A_{yy} .

I. INTRODUCTION

Recent applications of the (\vec{d}, γ) reaction to nuclear structure studies have given new insight on some of the D -state components of the ${}^3\text{He}$ wave function.^{1–4} A complete Faddeev calculation of the ${}^1\text{H}(\vec{d}, \gamma){}^3\text{He}$ reaction at $E_d = 30$ MeV using the Reid soft-core potential shows that practically all of the tensor analyzing power $A_{yy}(\theta)$ is due to a particular D -state configuration of ${}^3\text{He}$. This configuration consists of a correlated pair with internal relative orbital angular momentum $l=1$ with the third particle in a relative $l=1$ state with respect to the pair. Other reactions (e.g., sub-Coulomb pickup) are not sensitive to this particular component of the trinucleon wave function.⁵ When the Malfliet-Tjon potential (which does not have a tensor force) is used in place of the Reid soft-core potential, $A_{yy}(\theta)$ vanishes.¹

While the existence of a D -state component of the ${}^4\text{He}$ ground-state wave function has been known for some time from studies of forward dispersion relations,⁶ measurements of tensor polarized deuteron capture should give new information concerning the D -state components of the ${}^4\text{He}$ wave function. Previous experimental and theoretical investigations have been concentrated at deuteron laboratory energies between 150 keV and 50 MeV.^{7–12} The deuteron energy of our measurement is 95 MeV, chosen in large part since the charged particle telescopes and lead glass photon detectors have significantly better performance at higher energies. An additional reason for this choice of energy is to determine if the cen-

tral maximum in $\sigma(\theta)$ seen at higher energies ($E_d \approx 200$ – 376 MeV) is also present at $E_d = 95$ MeV.^{13,14} This maximum in the cross section is difficult to understand solely on the basis of direct deuteron capture. In addition to the cross section, the tensor analyzing power $A_{yy}(\theta)$ and vector analyzing power $A_y(\theta)$ were measured. These are the analyzing powers which can be measured if the alignment axis of the deuteron beam is perpendicular to the reaction plane, as is usually the case with a cyclotron.

The only allowed partial waves for the ${}^2\text{H}(\vec{d}, \gamma){}^4\text{He}$ reaction are those which have an even sum for the orbital and spin angular momentum quantum numbers, since the wave function must be symmetric due to the presence of identical bosons in the entrance channel. The spin independent component of the $E1$ multipole is forbidden by isospin conservation since ${}^4\text{He}$ is self-conjugate. The ${}^2\text{H}(\vec{d}, \gamma){}^4\text{He}$ reaction then proceeds predominantly through the $\langle {}^1D_2 | E2 | {}^1S_0 \rangle$ transition, with an angular distribution of $\sin^2\theta$ shape. At incident deuteron energies of about 2 MeV this transition begins to be suppressed because of the centrifugal barrier, and the cross section reflects the increasing importance of the 5S_2 partial wave.¹⁵ At very low energies ($E_d \approx 50$ keV) the angular distribution is practically isotropic, indicating a large contribution from the $\langle {}^5S_2 | E2 | {}^5D_0 \rangle$ transition involving the 5D_0 component of ${}^4\text{He}$.¹⁶

If only multipoles of rank two or less contribute, then there are eight allowed matrix elements. A complete decomposition of the reaction amplitude can be made if

the cross section and all analyzing powers (iT_{11} , T_{20} , T_{21} , and T_{22}) are measured. A complete measurement and analysis was carried out at $E_d \approx 10$ MeV, and it was found that the magnitudes of the vector and tensor analyzing powers were similar.⁸ This nonzero vector analyzing power is a signature of other multipoles besides the $E2$ multipole. It was noted that previously neglected mixing of the entrance channel partial waves by the tensor force destroys the unique relation between the entrance channel partial wave and the ${}^4\text{He}$ wave function. Recent calculations have shown that the assumption of direct capture for this reaction is flawed at low energy, with contributions from the $3+1$ partition (${}^3\text{He}+n$, ${}^3\text{H}+p$) being important in both the entrance channel and ${}^4\text{He}$ wave function.¹¹ The $3+1$ partition, for example, can masquerade as direct capture D -state effects even if the ${}^4\text{He}$ wave function is restricted to S -state components only.

II. THE EXPERIMENT

This measurement was carried out at the Indiana University Cyclotron Facility using a 95 MeV polarized deuteron beam. The experimental apparatus and data reduction techniques have been described in some detail in an earlier paper reporting our results for the ${}^1\text{H}(\vec{d}, \gamma){}^3\text{He}$ reaction.⁴ The vector polarization is typically $p_z = 0.28(\pm 0.01)$, and the tensor polarization is usually $p_{zz} = 0.82(\pm 0.04)$. The targets are CD_2 foils of thickness 11.9 ± 0.4 mg/cm².

Both the photon and the ${}^4\text{He}$ nucleus are detected, cleanly isolating the ${}^2\text{H}(\vec{d}, \gamma){}^4\text{He}$ events from the background. Eight lead glass Čerenkov detectors were used to detect the photons. Four detectors were placed on each side of the beam, and the angular range of the measurement was 48° – 144° in the laboratory. The solid angle was determined by a 7.62 cm lead collimator of either $10^\circ \times 15^\circ$ or $15^\circ \times 15^\circ$ acceptance. A 2.54 cm CH_2 absorber was placed in front of the collimator to absorb low energy charged particles. No anticoincidence detector was needed. These detectors had very good timing resolution (800 ps), but a pulse height resolution of only about 40% at 30 MeV. The recoiling ${}^4\text{He}$ nuclei are detected by plastic scintillator telescopes placed symmetrically on both sides of the deuteron beam. Each telescope consists of three plastic scintillator planes. The first plane is thin, giving excellent discrimination between charge $Z=1$ and charge $Z=2$ particles. The total thickness of the first and second plane is sufficient to stop all ${}^4\text{He}$ nuclei from the ${}^2\text{H}(\vec{d}, \gamma){}^4\text{He}$ reaction. The third scintillator plane was to have been used as a veto, but the particle identification is sufficiently good that the ${}^4\text{He}$ nuclei of interest can be separated on the basis of time of flight and pulse height correlations only. The three scintillator planes are summed to give a total pulse height in the recoil telescope. This ensures that the energy spectrum of the ${}^3\text{He}$ background (which does extend into the third plane) is treated in the same way as the ${}^4\text{He}$ events of interest.

Photons from the ${}^3\text{H}(\vec{d}, \gamma){}^4\text{He}$ reaction are identified by requiring a pulse height greater than 30 MeV with the proper time correlation relative to the rf pulse of the cy-

clotron. These photon conditions, along with a requirement that the pulse height in the first plane of the recoil telescope equal that of a helium nucleus, are then applied to a plot of charged particle flight time versus summed pulse height in the recoil telescope (Fig. 1). Note that while the four lead glass detectors of a side should give rise to four discrete peaks (shown by the arrows in Fig. 1) from the ${}^7\text{H}(\vec{d}, \gamma){}^4\text{H}$ reaction, two of the four peaks are merged together. The major component of the remaining background is ${}^3\text{He}$ nuclei from the ${}^2\text{H}(\vec{d}, \gamma){}^3\text{He}n$ reaction. A time of flight spectrum corresponding to each photon detector is generated from Fig. 1 by gating upon the total pulse height in the recoil telescope and projected onto the time axis. The yield of ${}^4\text{He}$ nuclei was then taken from a Gaussian fit to the peak. The ${}^3\text{He}$ background under the ${}^4\text{He}$ peak of interest was subtracted using a smooth extrapolation of the background on either side of the ${}^4\text{He}$ peak. The yield was corrected for deadtime using the measured computer deadtime. The event rate was low enough that the computer deadtime was the dominant contribution to the deadtime. The background due to random coincidences is subtracted by choosing events which had photons and helium nuclei in different beam bursts. The nonrandom background due to carbon in the CD_2 target (measured with a natural carbon target) is negligible. About 1% of all events are erroneously attributed to earlier beam bursts (an apparent shift to a shorter time of flight) due to random timing stops in the time digital converter (TDC), in good agreement with the expected shift based upon the singles rate in the first plane and the cyclotron rf frequency of 28.57 MHz.

The error budget for $\sigma(\theta)$ is shown in Table I. One of the major corrections was the subtraction of the ${}^3\text{He}$ background. The possible error in $\sigma(\theta)$ associated with this procedure is estimated to be about 5% in the central

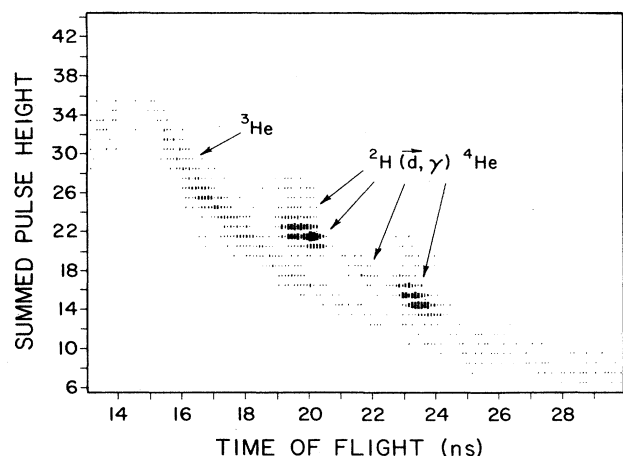


FIG. 1. The charged particle time of flight summed pulse height correlation in the charged particle telescope. This spectrum has been gated by photon time of flight and pulse height, and the first plane pulse height is required to be consistent with charge $Z=2$. The discrete grouping of the ${}^4\text{He}$ band is due to the kinematic correlation with the photon.

TABLE I. Systematic error budget for $\sigma(\theta)$, exclusive of target normalization.

Error source	$\theta=90^\circ, 99^\circ$ Uncertainty (%)	All other angles Uncertainty (%)
TDC shifts	0.75	0.75
Photon detector efficiency	2.0	2.0
Photon conversion in collimator	3.0	3.0
rf sorting cut	1.0	1.0
Reaction effects in telescope	1.0	1.0
${}^2\text{H}(\vec{d}, \gamma){}^3\text{He}n$ subtraction	5.0	3.0
Geometric effects: translation along axis	2.3	2.3
Geometric effects: non-normal collimator	2.5	2.5
Errors added in quadrature	7.2	6.0

minimum and 3% elsewhere. The efficiency correction due to ${}^4\text{He}$ reaction losses in the telescope is estimated using the total reaction cross section for ${}^4\text{He}$ nuclei incident upon carbon.¹⁷ The sorting loss due to a tight software window on the photon time of flight is 1%. This correction was measured by overconstraining the rf spectra with tight conditions from the recoil telescope. The efficiency of the Čerenkov detectors, including absorber effects, is estimated to be $96 \pm 2\%$ based upon measurements of the efficiency using tagged photons at the University of Illinois.¹⁸ The photon collimators are located to within an estimated uncertainty of 0.3 cm, giving an upward revision of $2.5 \pm 2.5\%$ to account for a possible nonnormal orientation of the collimator face, while an additional error of up to $\pm 2.3\%$ is possible due to a position uncertainty of the collimator along the target detector axis. Photon conversion in the inner edge of the collimator has been estimated to increase the true solid angle by 2% compared to the geometric solid angle.¹⁸ When all of these systematic uncertainties are added in quadrature, the total estimated error in the relative cross section is about $\pm 6.0\%$. The normalization of the cross section is uncertain to within about 4% because of the uncertainty in the deuterium content of the CD_2 target. A separate charged particle telescope of plastic and NaI scintillators was used to monitor the deuterium content of the CD_2 target. The deuterium content of the target decreases by about 1% per hour. Since targets are typically used for about eight hours, an average deuterium content of 96% of the initial value is chosen for the cross section calculation.

III. RESULTS

The results of this measurement are shown in Figs. 2–4. Systematic errors are included in the error estimates for $\sigma(\theta)$ only. These data are fit with Legendre functions using the minimization routine MINUIT.¹⁹ The fitted coefficients of these functions can be related to sums of

reaction matrix elements in a model independent way.²⁰ It should be noted that these analyses implicitly assume that the projectile has only an internal S state. In general, the cross section can be expanded as

$$\sigma(\theta) = A_0 \left[1 + \sum_{l=1} a_l Q_l P_l(\cos\theta) \right], \quad (3.1)$$

with $\sigma_{\text{tot}} = 4\pi A_0$. The Q_l are correction factors due to the finite aperture of the detector.^{21,22} In the plot of $\sigma(\theta)$ (Fig. 2), the solid line shows the best fit to the data including the effects due to finite detector aperture. The data points themselves have not been corrected for finite geometry effects. Also plotted in Fig. 2 is the $\sin^2 2\theta$ shape of a pure $\langle {}^1D_2 | E2 | {}^1S_0 \rangle$ transition normalized to

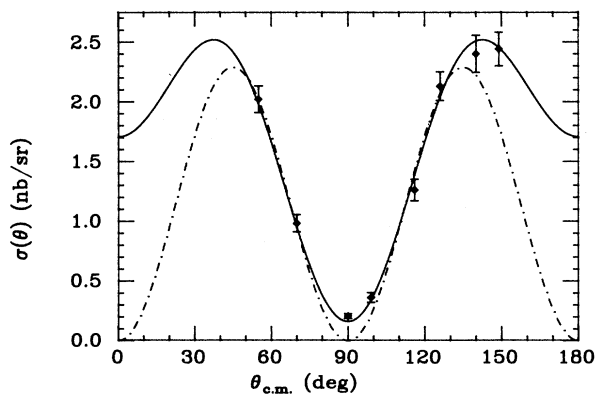


FIG. 2. Angular distribution $\sigma(\theta)$ for the ${}^2\text{H}(\vec{d}, \gamma){}^4\text{He}$ reaction. The solid line is a fit of Legendre polynomials (corrected for the finite detector aperture) to the data, while the dashed line is a $\sin^2(2\theta)$ curve normalized to the data at $\theta=55^\circ$. The error estimates include both statistical and systematic contributions, exclusive of a normalization uncertainty of 4%.

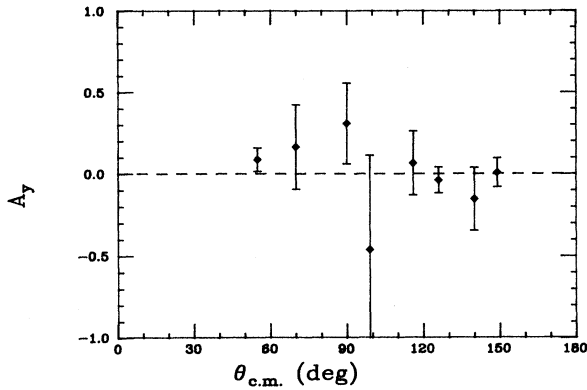


FIG. 3. The vector analyzing power A_y for the ${}^2\text{H}(\vec{d}, \gamma){}^4\text{He}$ reaction. The errors include only the statistical errors.

the data at $\theta=55^\circ$. Note that the central maximum observed at higher energies is not evident in our data. Because of the symmetry in the entrance channel, only the even polynomials contribute to the fit. If there are no multipoles of rank three or greater, then only the a_2 and a_4 coefficients are nonzero. The parameters of the fit are compared to the expansion coefficients for the pure $\langle {}^1D_2|E2|{}^1S_0 \rangle$ transition in Table II. Note that the magnitude of a_4 is significantly smaller than the $\langle {}^1D_2|E2|{}^1S_0 \rangle$ coefficient, while a_2 is roughly the same. The reduction of the magnitude of a_4 is a model independent signature of either $M2$ or additional $E2$ strength (i.e., non- $\langle {}^1D_2|E2|{}^1S_0 \rangle$), since only these multipoles can affect a_4 . These additional $E2$ components contribute via the tensor force. Also shown in Table II is the extracted value of A_0 from the fit. Using detailed balance, this value of A_0 gives a photodisintegration total cross section of $0.75 \pm 0.06 \mu\text{b}$ at $E_\gamma = 71 \text{ MeV}$ after division by two to account for the presence of identical particles in the exit channel.²³ Our value of σ_{tot} is in good agreement with other measurements in this energy range.²⁴

Our results for $A_y(\theta)$ and $A_{yy}(\theta)$ are shown in Fig. 3 and 4, respectively. The error estimates include only the statistical uncertainty, since the estimated systematic errors are much smaller.⁴ The measurement of $A_y(\theta)$ is less precise than the measurement of $A_{yy}(\theta)$ due to the low vector polarization of the deuteron beam. It is not possible to arrive at quantitative conclusions from this data set, since the coefficients of the Legendre expansion of $\sigma(\theta)A_y(\theta)$ and $\sigma(\theta)A_{yy}(\theta)$ are not sufficiently constrained by the data. It is possible to interpret some features of our data in a qualitative fashion if one neglects tensor force effects in the entrance channels. The quanti-

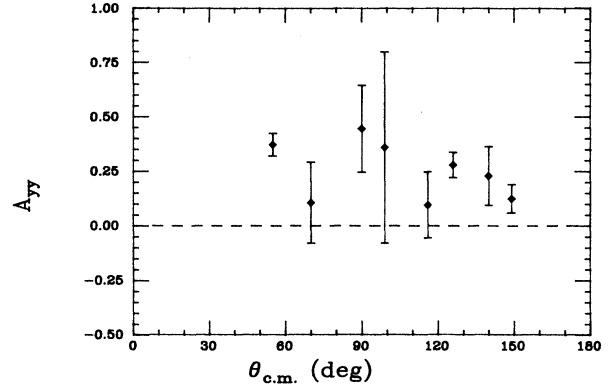


FIG. 4. The tensor analyzing power A_{yy} for the ${}^2\text{H}(\vec{d}, \gamma){}^4\text{He}$ reaction. The errors include only the statistical errors.

ty $\sigma(\theta)A_{yy}(\theta)$ was fit by an expansion of Legendre polynomials as

$$\sigma(\theta)A_{yy}(\theta) = 2A_0 \left[\sum_l c_l Q_l P_l(\cos\theta) \right], \quad (3.2)$$

where the factor of 2 is due to the tensor polarization asymmetry being $p_{yy}A_{yy}/2$ in Cartesian coordinates. The fit included terms through $l=4$ because of the presence of $E2$ - $E2$ interference terms. Although A_{yy} is a linear combination of both T_{20} and T_{22} , the first two coefficients of this expansion for $\sigma(\theta)A_{yy}(\theta)$ are related only to $\sigma(\theta)T_{20}(\theta)$. The c_0 and c_1 coefficients from the above expansion can be compared to those resulting from a sum of the matrix elements appropriate for T_{20} .²⁰ The only statistically significant coefficient of this data set was c_0 . The largest matrix element, $\langle {}^1D_2|E2|{}^1S_0 \rangle$, only appears in this coefficient as an interference with the $\langle {}^5D_2|E2|{}^5D_0 \rangle$ transition to the D state of ${}^4\text{He}$. In addition, the contribution of this interference to c_0 is significantly larger than those associated with the other contributions, which appear only as squared terms of these matrix elements. These non- $\langle {}^1D_2|E2|{}^1S_0 \rangle$ matrix elements are likely to be small, based on the shape of $\sigma(\theta)$. It is therefore likely that c_0 is dominated by this one interference term. Although a better χ^2 in the fit to $\sigma(\theta)A_{yy}(\theta)$ was found when odd components were allowed, both odd components in the fit through $l=4$ are not statistically significant. This odd component is interesting since it is due to either $E1$ or $M2$ (or both) transitions.²⁵ The presence of $E1$ or $M2$ transitions would also be confirmed by a nonzero vector analyzing power $A_y(\theta)$.

TABLE II. Expansion coefficients for $\sigma(\theta)$.

Coefficient	Fitted value and error	$\langle {}^1D_2 E2 {}^1S_0 \rangle$ transition
$A_0(\text{nb/sr})$	$+1.47 \pm 0.09$	
a_2	$+1.08 \pm 0.17$	0.714
a_4	-0.94 ± 0.24	-1.714

IV. CONCLUSIONS

Taken as a whole, our measurements indicate that the ${}^2\text{H}(\vec{d}, \gamma){}^4\text{He}$ reaction at $E_d = 95$ MeV is still dominated by the $\langle {}^1D_2 | E2 | S_0 \rangle$ transition. There are significant contributions from other transitions, as shown by the small value of the magnitude of a_4 in the fit to $\sigma(\theta)$. In contrast to the situation at lower energies, A_{yy} is much larger than A_y . The tensor analyzing power suggests that $E2$ transitions to the ${}^4\text{He}$ D state are important, although there may be some $E1$ or $M2$ strength reflected in the small fore/aft asymmetry in A_{yy} . Some $E1$ or $M2$ strength could also be allowed by the small value of A_y . As noted above, the presence of internal orbital angular momentum in the projectile (deuteron D state) must be ignored to reach these conclusions.

In the absence of a complete data set for all analyzing powers, one must use a model calculation in an attempt to interpret these data. At our energy the only available calculation for $A_{yy}(\theta)$ fails completely, even to the point of the wrong sign for $A_{yy}(\theta)$.²⁶ This particular calculation was carried out with the long wavelength and point deuteron approximations. The bound state wave function is adjusted to reproduce a realistic, variational ${}^4\text{He}$ wave function with correlations. Plane waves are used for the entrance channel, since at this energy the elastic channel data are very sparse. The assumption of a direct capture mechanism for this reaction may be fatally flawed, since even at lower energies it is known that the trinucleon-nucleon partition of the ${}^4\text{He}$ wave function is important.¹¹ At the higher energy and momentum transfer of this experiment it is likely that the reaction mechanism is even more sensitive to the trinucleon+nucleon partition of the ${}^4\text{He}$ ground state than at $E_d = 10$ MeV, since calculations of the ${}^4\text{He}$ ground-state wave function show that the $3+1$ partition is favored in the nuclear interior.²⁷ Qualitatively this would be due to the charge radius of ${}^2\text{H}$ being significantly larger than the charge radii of the $A = 3$ or 4 nuclei, and thus the interior of ${}^4\text{He}$ would resemble the $3+1$ partition more than the $2+2$ partition.

To begin to understand this reaction at intermediate

energies more new data is needed to extract the matrix elements. This requires the measurement of the vector analyzing power iT_{11} and the three tensor analyzing powers T_{20} , T_{21} , and T_{22} . More exotic observables such as spin correlation measurements are not needed in principle, since a complete multiple decomposition through $E2$ and $M2$ multipoles can be made using only analyzing power measurements. A less ambitious (but still worthwhile) measurement is to measure the vector analyzing power and at least one tensor analyzing power (either T_{20} or A_{yy}) to good precision. The vector analyzing power measurement would be sensitive to the $E1$ and $M2$ matrix elements, while the tensor analyzing power would also be sensitive to additional $E2$ components. This assumes that there is no contribution of rank 3 or higher. Such rank three components would give a term proportional to P_6 in $\sigma(\theta)$, and limits could be set on the presence of such terms from a precise measurement of $\sigma(\theta)$. The simplest course (and perhaps the best) would be to use the existing apparatus with a pure vector polarized beam. This would result in nearly an order of magnitude improvement in the figure of merit for A_y . This new measurement would be very sensitive to the isospin suppressed $E1$ transition. This new result, with the existing A_{yy} data, could be used to test model calculations of this reaction. Without the impetus provided by new calculations, however, it is difficult to justify additional measurements.

ACKNOWLEDGMENTS

Always useful discussions with A. Arriaga, W. Haeberli, F. D. Santos, and J. A. Tostevin are gratefully acknowledged. The assistance and cooperation of P. T. Debevec, S. Lebrun, and A. M. Nathan of the University of Illinois with the tests of the photon detectors was very much appreciated. S. W. Wissink's assistance with the multipole analysis was crucial. C. S. Yang and V. R. Cupps contributed to the early stages of this work. Support was furnished by the National Science Foundation as part of Grant 84-12177.

*Present address: University of Wisconsin, Madison, WI 53706.

†Present address: Princeton University, Princeton, NJ 08544.

‡Present address: Los Alamos National Laboratory, Los Alamos, NM 87545.

§Present address: Fluehwiesenweg 5, CH-8116 Wuerenlos, Switzerland.

**Present address: University of North Carolina, Chapel Hill, NC 27514.

††Present address: University of Bonn, Bonn, FRG.

‡‡Permanent address: University of The Western Cape, Belleville, South Africa.

¹J. Jourdan, M. Baumgartner, S. Burzynski, P. Egelhof, A. Klein, M. A. Pickar, G. R. Plattner, W. D. Ramsey, H. W. Roser, I. Sick, and J. Torre, Phys. Lett. **162B**, 269 (1986); J. Jourdan, M. Baumgartner, S. Burzynski, P. Egelhof, R. Hen-

neck, A. Klein, M. A. Pickar, G. R. Plattner, W. D. Ramsey, H. W. Roser, I. Sick, and J. Torre, Nucl. Phys. **A453**, 220 (1986).

²M. C. Vetterli, J. A. Kuehner, A. J. Trudel, C. L. Woods, R. Dymarz, A. A. Pilt, and H. R. Weller, Phys. Rev. Lett. **54**, 1129 (1985).

³A. Arriaga and F. D. Santos, Phys. Rev. C **29**, 1945 (1984).

⁴W. K. Pitts, H. O. Meyer, L. C. Bland, J. D. Brown, R. C. Byrd, M. Hugi, H. J. Karwowski, P. Schwandt, A. Sinha, J., Sowinski, I. J. van Heerden, A. Arriaga, and F. D. Santos, Phys. Rev. C **37**, 1 (1988).

⁵T. E. O. Ericson and N. Lo Iudice, Nucl. Phys. **A475**, 199 (1987).

⁶G. R. Plattner, R. D. Viollier, and K. Alder, Phys. Rev. Lett. **34**, 830 (1975).

- ⁷H. R. Weller, P. Colby, N. R. Roberson, and D. R. Tilley, *Phys. Rev. Lett.* **53**, 1325 (1984).
- ⁸S. Mellema, T. R. Wang, and W. Haeberli, *Phys. Lett.* **166B**, 282, (1986); *Phys. Rev. C* **34**, 2043 (1986).
- ⁹F. D. Santos, A. Arriaga, A. M. Eiró, and J. A. Tostevin, *Phys. Rev. C* **31**, 707 (1985); A. Arriaga, A. M. Eiró, F. D. Santos, and J. E. Ribeiro, *ibid.* **37**, 2312 (1988).
- ¹⁰J. A. Tostevin, *Phys. Rev. C* **34**, 1497 (1986).
- ¹¹B. Wachter, T. Mertelmeier, and H. M. Hofmann, *Phys. Lett. B* **200**, 246 (1988).
- ¹²H. R. Weller, R. M. Whitton, J. Langenbrunner, Evans Hayward, W. R. Dodge, S. Kuhn, and D. R. Tilley, *Phys. Lett. B* **213**, 413 (1988).
- ¹³B. H. Silverman, A. Bourad, W. J. Briscoe, G. Bruge, P. Couvert, L. Farvacque, D. H. Fitzgerald, C. Glasshauser, J.-C. Lugol, and B. M. K. Nefkens, *Phys. Rev. C* **29**, 35 (1984).
- ¹⁴J. Arends, J. Eyink, T. Hegerath, H. Hartmann, B. Mecking, G. Noldeke, and H. Rost, *Phys. Lett. B* **62**, (1984).
- ¹⁵H. R. Weller, P. Colby, J. Langenbrunner, Z. D. Huang, D. R. Tilley, F. D. Santos, A. Arriaga, and A. M. Eiro, *Phys. Rev. C* **34**, 32 (1986).
- ¹⁶C. A. Barnes K. H. Chang, T. R. Donoghue, C. Rolfs, and J. Kammeraad, *Phys. Lett. B* **197**, 315 (1987).
- ¹⁷R. M. DeVries and J. C. Peng, *Phys. Rev. C* **22**, 1055 (1980).
- ¹⁸M. A. Pickar, Ph.D. thesis, Indiana University (1982).
- ¹⁹F. James and M. Roos, *Comp. Phys. Commun.* **10**, 343 (1975).
- ²⁰R. G. Seyler and H. R. Weller, *Phys. Rev. C* **20**, 453 (1979).
- ²¹M. E. Rose, *Phys. Rev.* **91**, 610 (1953).
- ²²W. K. Pitts, Ph.D. thesis, Indiana University, 1987.
- ²³W. E. Meyerhof, W. Feldman, S. Gilbert, and W. O'Connell, *Nucl. Phys.* **A131**, 489 (1969).
- ²⁴Yu. M. Arkatov, P. I. Vatsset, V. I. Voloshchuk, I. M. Prokhorets, A. F. Khodyachikh, and V. I. Chmil', *Yad. Fiz.* **16**, 12 (1972) [*Sov. J. Nucl. Phys.* **16**, 6 (1973)].
- ²⁵R. G. Seyler and H. R. Weller, *Phys. Rev. C* **31**, 1952 (1985).
- ²⁶J. A. Tostevin, private communication.
- ²⁷H. Kanada, T. Kaneko, and Y. C. Tang, *Phys. Rev. C* **34**, 22 (1986).